Δελτίο της Ελληνικής Γεωλογικής Εταιρίας, τομ. XLVII , 2013
Πρακτικά 13ου Διεθνούς Συνεδρίου, Χανιά, Σεπτ. 2013

Bulletin of the Geological Society of Greece, vol. XLVII 2013
Proceedings of the 13th International Congress, Chania, Sept. 2013

COSEISMIC STRESS DISTRIBUTION ALONG ACTIVE STRUCTURES AND THEIR INFLUENCE ON TIME-DEPENDENT PROBABILITY VALUES

Paradisopoulou P.[1], Papadimitriou E.[1], Mirek J.[2] and Karakostas V.[1]

[1] *Geophysics Department, School of Geology, Aristotle University of Thessaloniki, GR54124, Thessaloniki, Greece, ppara@geo.auth.gr, ritsa@geo.auth.gr, vkarak@geo.auth.gr*

[2] *Faculty of Geology, Geophysics and Environmental Protection, AGH University of Science and Technology, Krakow, Poland, jmirek@seismo.geol.agh.edu.pl*

Abstract

Based on the fact that stress changes caused by the coseismic slip of strong events can be incorporated into quantitative earthquake probability estimates, the goal of this study is to estimate the probability of the next strong earthquake (M≥6.5) on a known fault segment in a future time interval (30 years). The probability depends on the calculation of ΔCFF and the estimate of the occurrence rate of a characteristic earthquake, conditioned to the elapsed time since the previous event. The Coulomb stress changes caused by previous earthquakes are computed and their influence are considered by the introduction of a permanent shift on the time elapsed since the previous earthquake or by a modification of the expected mean recurrence time. The occurrence rate is calculated, taking into account both permanent and temporary perturbations. The estimated probability values correspond to the probabilities along each fault segment with discretization of 1km, illustrating the probability distribution across the specific fault. In order to check whether the estimated probability vary with depth, all the estimations were performed for each fault at depths of 8, 10, 12 and 15 km.

Key words: *Faults, strong earthquakes, renewal process, Greece.*

Περίληψη

Στόχος της παρούσας εργασίας είναι η εκτίμηση της πιθανότητας γένεσης ισχυρών σεισμών (M≥6.5) στα ενεργά ρήγματα της Ελλάδας και της ευρύτερης περιοχής της. Πιο συγκεκριμένα δίνεται η κατανομή της πιθανότητας κατά μήκος και ανά 1km σε κάθε ενεργό δομή που συνδέεται με κάποιο ισχυρό σεισμό (M≥6.5). Για να γίνει εκτίμηση της πιθανότητας λήφθηκε υπόψη η μεταβολή της τάσης που προκύπτει μετά από κάθε ισχυρό σεισμό και η οποία έχει ως αποτέλεσμα να επιταχύνει ή να επιβραδύνει τη γένεση ενός επόμενου σεισμού. Γίνεται δηλαδή ενσωμάτωση των μεταβολών των τάσεων στη χρονικά εξαρτώμενη πιθανότητα, με σκοπό να δειχθεί κατά πόσο μία μεταβολή στην τάση συμβάλλει στη διαδικασία του να γίνει ένας σεισμός σ' ένα ρήγμα. Το μοντέλο της δεσμευμένης πιθανότητας είναι αυτό που χρησιμοποιήθηκε για τους υπολογισμούς οι οποίοι γίνονται για τα επόμενα 30 χρόνια. Οι υπολογισμοί πραγματοποίηθκαν σε διάφορα βάθη (8, 10, 12 και 15km) για να ελεγχθεί κατά πόσο μεταβάλλονται οι τιμές των πιθανοτήτων, οι οποίες παρουσιάζονται σε χάρτες για την άμεση οπτική αντίληψη της χωρικής κατανομής τους.

Λέξεις κλειδιά: *Ενεργά ρήγματα, ισχυροί σεισμοί, περίοδος επανάληψης, Ελλάδα.*

1. Introduction

Studying the distribution of strong (M>6.5) historical and recent earthquakes it is found that they may occur on the same fault (after a time recurrence) or in adjacent faults activated by previous earthquakes. Fault interaction along with the time and space where an earthquake can occur led to the development of many methodologies, one of which being the incorporation of stress changes to the calculation of earthquake probabilities. The so-called Coulomb stress changes resulting from coseismic slip strongly affect the time and the location of subsequent events (mainshocks or aftershocks) making stress changes a useful tool for indentifying risk areas.

The field of time dependent models for earthquake probability estimations were introduced, based on various geologic and geophysical data such as fault slip rates, the interevent times of prior strong earthquakes (e.g., Working Group on California Earthquake Probabilities, 1990). Stress triggering and fault interaction are also starting to be incorporated into time-dependent earthquake probability estimates by Stein et al., 1997; Toda et al., 1998; Working Group on California Earthquake Probabilities, 1999; Parsons et al., 2000.

Following these methodologies Paradisopoulou et al. (2010a) used 67 strong earthquakes ($M \geq 6.5$) that occurred in Greece and its adjacent areas since the beginning of 20th century (instrumental era) and calculated the coseismic stress changes due to these earthquakes. Incorporating the effect of stress change into the time–depended probability estimates using an earthquake nucleation constitutive relation, which includes both permanent and transient effects of stress changes the probability during the next years, was calculated in each known fault of the study area. The present study is a step forward in the application of the same methodology. The goal here is to calculate probabilities along each fault of the study area with discretization of 1km, illustrating the probability distribution across the specific fault. In order to demonstrate whether the estimated probabilities vary with depth, all calculations were performed in each case at depths of 8, 10, 12 and 15 km. Probability calculations were carried out and given for the entire study area during the next 30 years.

2. Coseismic Stress Changes

Static stress change is a mechanism of earthquake triggering. “Triggering” has the meaning that one earthquake causes another earthquake which would not have otherwise occurred at that time. Rupture perturbs the state of stress on neighboring faults that in turn “encourages” or “suppresses” earthquakes on adjacent faults depending on the increase or decrease of stress. Our study uses the assumption that an earthquake can be modeled as a moving dislocation in an elastic half space (Okada, 1992) enabling estimation of stress transfer to other faults. Earthquakes occur when stress exceeds the strength of the fault. The closeness to the failure is quantified using the change in Coulomb failure function (ΔCFF). The Coulomb failure stress change is given by eq. 1:

Equation 1 - Coulomb failure stress change formulation

$$\Delta CFF = \Delta\tau + \mu(1 - B)\Delta\sigma$$

where $\Delta\tau$ is the change in shear stress on a fault, $\Delta\sigma$ is the change in normal stress, μ is the friction coefficient and B is the Skempton’s coefficient (in this study we assume μ =0.75 and B=0.5 as in Robinson and McGinty, 2000 among others). $\Delta\sigma$ and $\Delta\tau$ are calculated for a fault plane at the observing (field) point. For increasing shear stress in the direction of relative slip on the observing fault $\Delta\tau$ is positive. $\Delta\sigma$ is positive for tensional normal stress. The shear modulus and Poisson’s ratio are fixed at $3.3 \cdot 10^5$ bar and 0.25, respectively. Coulomb stress changes are calculated according to the geometry of the target fault, which is the fault of the anticipated strong earthquake, and at the appropriate depth. In our study area it is known that the majority of the foci of the

crustal earthquakes are located in the depth range of 3 to 15 km, which defines the brittle part of the crust. Considering all the above information the seismogenic layer in our calculations is taken to be in this range for all the strong events (M≥6.5) modeled.

3. Earthquake Probability Estimation

In this section we estimate the probabilities for the occurrence of future strong (M>6.5) events along the fault segments associated with events of M>6.5 that occurred either during the instrumental period or in the past centuries and for which information exists. The adequate proposed methodology followed is that by Stein et al. (1997), Toda et al. (1998) and Parsons (2000, 2004, 2005) who support an earthquake renewal process in which the probability of a future event grows as the time of previous event increases considering both permanent and transient effects of the stress changes on earthquake probabilities. To calculate such a renewal probability, ideally, one needs an earthquake catalog containing several strong events on each fault to deduce earthquake magnitudes, the mean interevent time of similar events, and the elapsed time since the last shock on each fault.

3.1. Probability Models

Two models for earthquake probabilities estimates are generally in use: the stationary Poisson model and the conditional probability model (Cornell et al., 1968; Hagiwara, 1974). Using both of the mentioned models we estimate the probability of an earthquake to occur in the next 30 years from 2012.

Poisson model: This model is one that treats earthquakes as occurring randomly in time (t) about a mean recurrence interval (T_r). The probability of at least one event in the time interval (t, t+Δt) is given by:

Equation 2 - Poisson probability model

$$P(t \le T \le t + \Delta t) = 1 - e^{-\Delta t / T_r}$$

Conditional Probability model: This model is time-dependent and includes knowledge of the time elapsed since the last event and may also include the effects of a given stress change. Following Working Group of California Earthquake Probabilities (1988) the probability that an earthquake will occur at time T in the interval (t, t+Δt) is:

Equation 3 - Conditional probability formulation

$$P(t \le T \le t + \Delta t) = \int_t^{t+\Delta t} f(t)dt$$

Where f(t) is the probability density function for the earthquake occurrence. We assume a lognormal probability distribution of recurrence time (e.g. Nishenko and Buland, 1987):

Equation 4 - Probability density function for lognormal distribution

$$f(t, \alpha, \beta) = \frac{1}{\beta t \sqrt{2\pi}} \exp\left[\frac{-(\ln \frac{t}{\alpha})^2}{2\beta^2} \right]$$

where $\beta^2 = \ln(\frac{s_t^2}{T_r^2} + 1), \alpha = \ln\left[T_r \exp(-0.5\beta^2)\right]$, T_r is the average interevent time, s_t: the standard deviation of interevent time. The probability conditioned on the fact that the earthquake has not occurred prior to t is:

Equation 5 - Conditional probability (an earthquake not occurring prior to t)

$$P(t \le T \le t + \Delta t \mid T > t) = \frac{P(t \le T \le t + \Delta t)}{P(T \ge t)}$$

3.2. Incorporating Stress Changes into Earthquake Probability Calculations

3.2.1. Permanent effect of stress change: To include the permanent effect of a stress change (ΔCFF), an assumption is made that a sudden stress increase (or decrease) linearly shortens (or lengthens) the time until the next earthquake. The advance or delay, termed a clock change (T′), can be calculated by dividing the stress change by the tectonic stressing rate ($\dot{\tau}$): T′=ΔCFF/ $\dot{\tau}$. Thus, an adjusted time by the clock change is taking into account and the conditional probability is now equal to:

Equation 6 - Static probability change formulation

$$P_c(t_1) = \frac{\int_{t_1}^{t_1+\Delta t} f_t(t + T')dt}{\int_{t_1}^{\infty} f_t(t + T')dt}$$

3.2.2. Transient probability change: The method is based on the model of Dieterich (1994), which incorporates changes in stress caused by a prior earthquake to changes in seismicity rate. The transient change in expected earthquake rate R(t) after a stress step can be related to the probability of an earthquake of a given size over the time interval Δt (30 years in this study) through a non stationary Poisson process as (Dieterich and Kilgore, 1996):

Equation 7 - Transient probability change formulation

$$P(t, \Delta t) = 1 - \exp\left[-\int_t^{t+\Delta t} R(t)dt\right] = 1 - \exp\left[-N(t)\right]$$

Integrated for N(t) yields:

Equation 8 - The expected number of earthquakes in the interval Δt

$$N(t) = r_p \left\{ \Delta t + t_\alpha \ln \left[\frac{1 + \left[\exp(-\frac{\Delta CFF}{A\sigma}) - 1 \right] \exp\left[\frac{-(\Delta t)}{t_\alpha} \right]}{\exp\left(\frac{-\Delta CFF}{A\sigma} \right)} \right] \right\}$$

Where t_α is the characteristic duration of the transient effect, σ, is the normal stress, A, is a fault constitutive constant and ΔCFF is the calculated Coulomb stress change. Note that the transient effect disappears if ΔCFF=0, that is $N=r_p \cdot \Delta t$. r_p is the expected rate of earthquakes associated with the permanent probability change (Toda et al., 1998). This rate can be determined again by applying a stationary Poisson probability expression as:

Equation 9 - Permanent background component of earthquake rate

$$r_p = -\frac{1}{\Delta t} \ln\left[1 - P_c\right]$$

where P_C is the conditional probability taken from eq. 6.

4. Input Parameter Calculations

Mean interevent time (T_r). For the calculation of time dependent probability of an earthquake of a given magnitude (in our case M≥6.5 under the renewal model), it is necessary to know or to estimate the mean interevent time and the time elapsed since the last earthquake of comparable size. These parameters are most commonly drawn from historic and paleoseismic record. Historical information is mainly taken from Papazachos and Papazachou (2003), Ambraseys and Jackson (2000) and Ambraseys (2002). For some faults information is taken from specific published works and used for assigning T_r onto them. Results on paleoseismic records on the North Anatolian Fault (NAF) are given by Rockwell et al. (2001), Klinger et al. (2003), Parsons, 2004, Palyvos et al. (2007), Pondard et al. (2007), Kurcer et al. (2008), Pantosti et al. (2008), which support Tr~207 - 275years. In the area of Corinth Gulf, for Eliki's (S43) and Xylokastro (S44) fault, mean interevent times of 242±60 and 119±20 years, respectively, was found (Briole et al., 2000; Koukouvelas et al. 2001). Collier et al. (1998) give a calculated mean interevent time equal to 330 years. Pavlides et al. (2004) suggest a mean interevent time of 1000 years on Atalanti's fault whereas Pantosti et al. (2004) estimated for the same fault 660-1200 years (faults S59-S61). In cases where only one or two events were reported for a particular fault segment, the interevent times are set equal to 500 years.

Rate and state parameters. Two parameters must be chosen for use of the rate- and state-dependent model of Dieterich (1994). The one is the tectonic stressing rate ($\dot{\tau}$) which is obtained directly from the chosen yearly slip rate for each fault segment. For parts of North Anatolian Fault, is found equal to 0.04-0.25bar/yr with a mean value 0.10 bar/yr. These values are in agreement with the ones from Stein et al. (1997), who estimated a value of 0.15bar/yr along most of the NAF system and from Parsons et al. (2000) and Parsons (2004) who proposed 0.1-0.064 bar/yr. For the remaining part of the study area the values of stressing rate are in the range of 0.003-0.25 bar/yr.

The second parameter is the duration of transient effect t_α. Following Dieterich (1994) we set t_α equal to 10% of the minimum mean interevent time. Thus, for the area of North Anatolian fault t_α=25 yr, considering a minimum return period of 250 years. For the same area a regional aftershock decay time for M>6.7 earthquakes was found to be ~35 years by Parsons et al. (2000). A value of t_α=50 yr was set for the rest part of our study area due to the longer observed interevent times (~ 500 years). For the southern part of Corinth Gulf the t_α was set equal to 30 years and for the Ionian Sea equal to 10 years due to the more frequent occurrence of such events in these areas.

5. Discussion and Conclusions

Until now the probability estimations were performed (Paradisopoulou et al., 2010a, b) for one value (minimum, maximum or average) of ΔCFF not allowing us to discriminate the exact location of this value on the fault (Figure 1). In this study, probabilities are calculated taken into account Coulomb stress changes along each fault at points with 1km spacing between them, and in four different depths onto the fault, thus giving us the advantage to observe the probability value and the stress influence at every fault patch.

5.1. Assumptions on Calculations

Some assumptions are made in this study and concern both stress calculation and probability estimation. At the outset, all stress calculations are performed in a homogeneous elastic half space and require a coefficient of friction (μ) and the Skempton's coefficient (B). An additional assumption of stress change calculation uncertainty is the dip and rake angles of the target fault which are known approximately, e.g. from surface projection, or they are defined from structural information or by moment tensors or focal mechanisms. In all cases there are uncertainties that lead to variation in stress change calculations. An effort was made in order to investigate to which extend the uncertainties, involved in the fault parameters, influence the calculated stress pattern by Paradisopoulou et al. (2010a). The correlation between calculated stress changes and different val-

ues of Skempton's coefficient (B), rake and dip angle of the fault are tested following the technique of Parsons (2005).

To pass from stress changes to probability estimations a second set of assumptions was done based on historical, paleoseismic data (needed for the calculation of T_r and elapsed time) and geodetic data (required for estimation of stressing rate, $\dot{\tau}$). These assumptions are necessary for the permanent probability change calculation due to advance or delay of time until the next earthquake. The conditional probability model using, in our case, the lognormal distribution, intrinsically involves uncertainties on the mean earthquake interevent time (T_r) and on the elapsed time.

For the dominant transient effect of the stress changes on earthquake probability, rate-state constitutive relations were applied, which require parameters such as t_α (aftershock duration) and Aσ (a state parameter). We assume, according to seismicity of each subarea of the study area and the mean recurrence time (Dieterich, 1994) that t_α is equal to 10% of T_r. With given values of the parameters t_α and $\dot{\tau}$, the Aσ was calculated using the equation: $A\sigma=t_\alpha \cdot \dot{\tau}$. The stressing rate $\dot{\tau}$ is related with the time, T΄, and therefore it could for example lead to smaller clock changes for a given stress change, and hence to smaller probability values. For this reason several values of $\dot{\tau}$ were used for each fault zone as already mentioned.

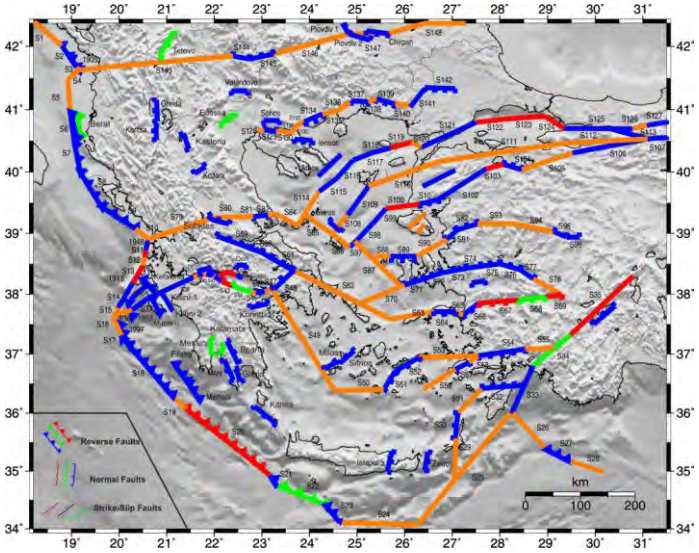

Figure 1 - Map of estimated time dependent probabilities for the occurrence of an earthquake with magnitude M≥6.5 for the next 30 years (after 2009), on each fault segment of the study area (modified from Paradisopoulou et al., 2010b). High probabilities are shown with red color, and lower values with green and blue colors. Orange color is corresponding to the faults for which no probability value is estimated.

5.2. Results

Detailed earthquake occurrence probabilities are provided by gridding the target fault areas and performing calculations on the nodes of the grid spacing 1km (Figures 2). In these figures, green colors denote faults where the probability values are low (P<0.09) due mostly to the effect of negative changes in Coulomb stress. Yellow to red colors represent higher probability values (0.09 ≤ P < 0.30 and P≥0.30, respectively) due mainly to positive ΔCFF values on these faults. The entirely green lines represent faults that have already failed whereas red lines correspond to faults that are candidate to host an incoming earthquake. Additionally to the effect of stress step (ΔCFF), rate and state parameters such as the duration of transient effect (t_α), the stressing rate ($\dot{\tau}$), mean interevent time (T_r) and elapsed time have influence to the results. Thus, for some faults illustrated

by yellow to red (or green) color, the probability changes are generally significant (or negligible) only for time intervals which are short (or long) compared to the repeat time of the fault. As far as the depth dependence concerns, there are no significant differences between the values corresponding to different chosen depths (e.g. ±0.03 for S122, ± 0 for S123, ± 0.016 for S124, ± 0 for 125, ± 0.0016 for Tetovo and ± 0.046 for SW Crete).

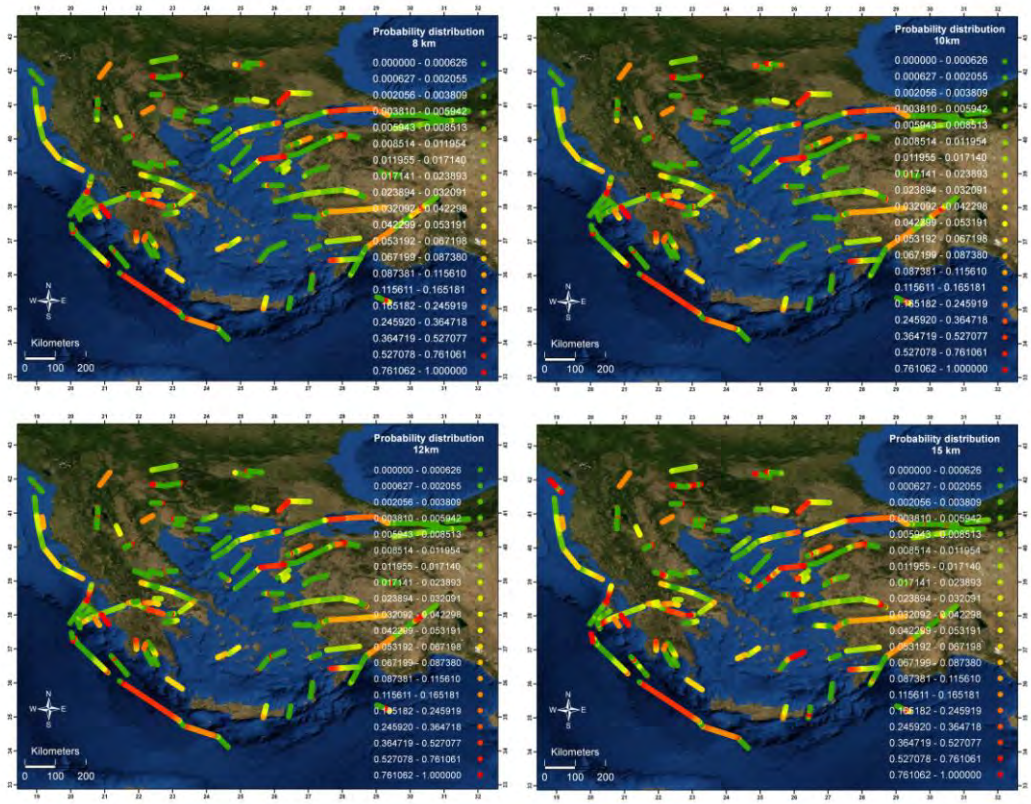

Figure 2 – Probability distribution along each fault of the study area. Calculations were performed at 8km, 10 km, 12km and 15km depth. Colors between green and yellow correspond to low probability values (P<0.09) and colors between yellow and red indicate higher probability values (0.09 ≤ P < 0.30 and P≥0.30).

Observing the probability values (Figure 2), unusually high ones (red color) were found at the edges of some faults. More precisely, neighbouring faults such as S95–S96, S122-S123-S124, S144 – S145, Plovdiv 2 – Chirpan, Sohos – S129 and individual faults such as Filiatra, Ohrida, S125, Valandovo, Kozani, S30, S35, S37, S77, S82, display low probability values while the faults boundaries exhibit one or more values that exceed the 80%. These values are uncertainties that introduced to the calculations due to the effect of stress changes. The method of calculating probabilities with the use of 1km grid onto the fault, enabling us to reduce any contingency to the estimated values. Figure 3 exemplifies the graphs of 30-years conditional probability along the fault, for six segments (S22 (south Crete), S122, S123, S124, S125 (Izmit) and S144 faults). The counting on x-axis starts from the left edge of each fault. All plots represent a further illustration (addition to Figure 2) of probability grid along the faults. Taking into account the above, the following results may be drawn:

a) There are some distinct values which can contaminate our results; therefore they can easily be removed for calculation improvement. Notice that these discrete values are observed at the fault boundaries (focus for example on S22 fault) and see in more detail

that the probabilities are under the influence of stress transfer between adjacent faults. S22 fault is located between two faults that have already ruptured and hence large values of ΔCFF and consequently higher probability values displayed at S22 edges.

b) Generally the probability results are more correctly and acceptable due to fact that there is a range of estimated probability values onto the fault instead of one value (minimum, maximum, average). On S122 fault for example (at 10 km depth) probability values ranging from 0.008 to 0.40 and 0.50 at the most part of the fault, while 0.38 was the estimated mean probability for the entire fault using the average value of ΔCFF on permanent and transient effect.

Consequently the methodology used could be useful for identifying those areas or cities with enhanced probability for large and damaging mainshocks. Additionally if the aforementioned assumptions will be reduced the estimation of the earthquake probabilities has profound implications for seismic hazard analysis.

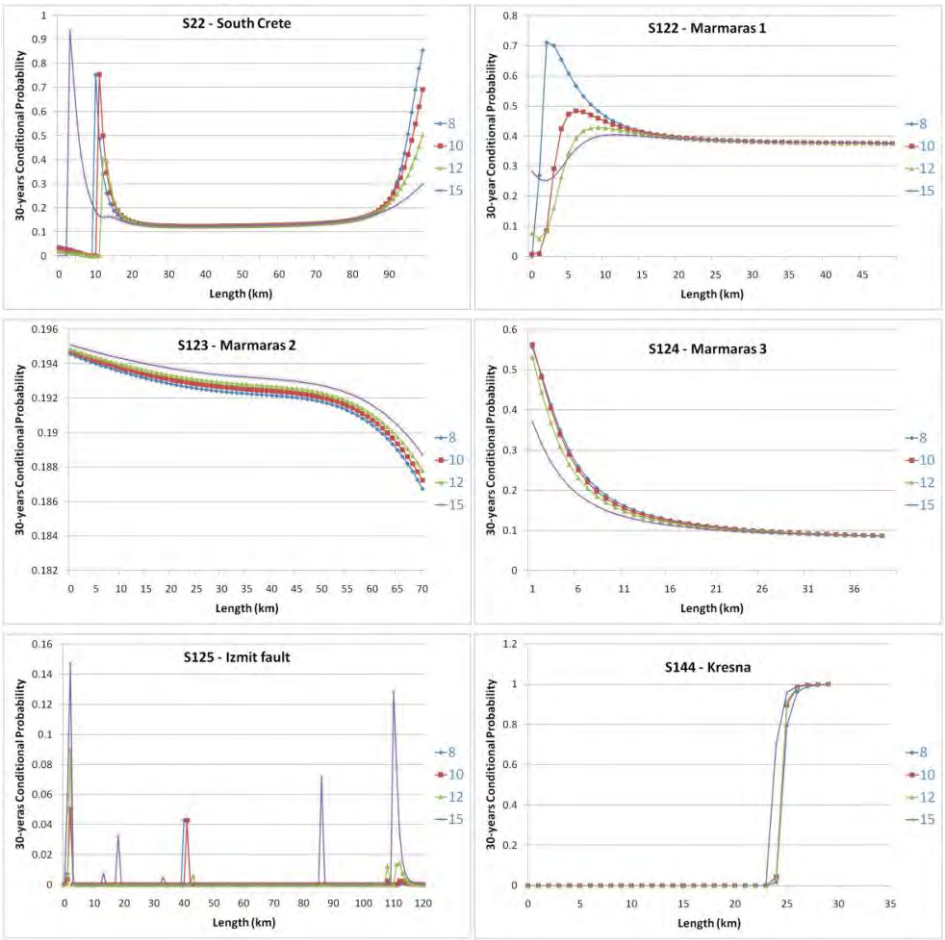

Figure 3 - Graph of 30 years estimated probability values along the strike of the fault for six faults of our data sample, indicating the uncertainties and singularities in probability distrib ution along the fault.

6. Acknowledgments

The stress tensors were calculated using a program written by J. Deng (Deng and Sykes, 1997) based on the DIS3D code of S. Dunbar, which later improved (Erikson, 1986) and the expressions of G. Converse. Maps are from ESRI. This work was partially supported by the research project 11.11.140.767 financed by the Polish State Committee for Scientific Research, AGH University of Science and Technology, Faculty of Geology, Geophysics and Environmental Protection. Geophysics Department contribution number 810.

7. References

Ambraseys N.N. 2002. The seismic activity of the Marmara Sea region over the last 2000 years, *Bulletin Seismological Society of America*, 92, 1-18.

Ambraseys N.N. and J. A. Jackson 2000. Seismicity of Marmara (Turkey) since 1500, *Geophysical Journal International,* 141, F1-F6.

Briole P., Rigo A. Lyon-Caen, H. Ruegg J.C., Papazissi K., Mitsakaki C., Balodimou A., Veis G., Hatzfeld D. and Deschamps A. 2000. Active deformation of the Corinth rift, Greece: Results from repeated Global Positioning System surveys between 1990 and 1995, *Journal of Geophysical Research 105, 605-625.*

Collier, R. E., Pantosti D., D'addezio G., De Martini P.M., Masana E. and Sakellariou D. 1998. Paleoseismicity of the 1981 Corinth earthquake fault: seismic contribution to extensional strain in central Greece and implications for seismic hazard, *Journal of Geophysical Research* 103, 30001-30019.

Cornell C.A., Wu S.C., Winterstein S.R., Dieterich J.H. and Simpson R.W. 1968. Seismic hazard induced by mechanically interactive fault segments, *Bulletin Seismological Society of America* 83, 436–449.

Dieterich J.H. 1994. A constitutive law for rate of earthquake production and its application to earthquake clustering, *Journal of Geophysical Research,* 99, 2601–2618.

Dieterich J. H. and Kilgore B. 1996. Implications of fault constitutive properties for earthquake prediction, *Proceedings of the National Academy of Sciences U.S.A,* 93, 3787–3794.

Hagiwara Y. 1974. Probability of earthquake occurrence as obtained from a Weibull distribution analysis of crustal strain, *Tectonophysics,* 23, 313-318.

Klinger Y., Sieh, K., Altunel, E., Akoglu, A., Barka A., Dawson T., Gonzalez T., Meltzner A. and Rockwell T. 2003. Paleoseismic Evidence of Characteristic Slip on the Western Segment of the North Anatolian Fault, Turkey, *Bulletin of Seismological Society of America,* 93, 2317–2332.

Koukouvelas I.K., Stamatopoulos L., Katsanopoulou D. and Pavlides S. 2001. A palaeoseismological and geoarchaeological investigation of the Eliki fault, Gulf of Corinth, Greece, *Journal of Structural Geology,* 23, 531-543.

Kurcer A., Chatzipetros A., Tutkun S. Z., Pavlides S., Ates O. and Valkaniotis S. 2008. The Yenic Gonen active fault (NW Turkey): Active tectonics and palaeoseismology, *Tectonophyics* 453, 263–275.

Nishenko S. P. and Buland R. 1987. A generic recurrence interval distribution for earthquake forecasting, *Bulletin Seismological Society of America*, 77, 1382–1399.

Okada Y. 1992. Internal deformation due to shear and tensile faults in a half space, *Bulletin of Seismological Society of America,* 82, 1018-1040.

Palyvos N., Pantosti D., Zabci C. and D' Addezio G. 2007. Paleoseismological evidence of recent earthquakes on the 1967 Mudurnu valley earthquake segment of the North Anatolian Fault zone, *Bulletin Seismological Society of America,* 97, 1646–1661.

Pantosti D., De Martini P.M., Papanastassiou D., Lemeille F., Palyvos N. and Stavrakakis G. 2004. Paleoseismological Trenching across the Atalanti Fault (Central Greece): Evidence for the Ancestors of the 1894. Earthquake during the Middle Age and Roman Times, *Bulletin Seismological Society of America,* 94, 2, 531-549.

Pantosti D., Pucci S., Palyvos N., De Martini P.M., D' Addezio G., Collins P.E.F. and Zabci C. 2008. Paleoearthquakes of the Düzce fault (North Anatolian Fault Zone): Insights for large surface faulting earthquake recurrence, *Journal of Geophysical Research* 113, doi: 10.1029/2006JB004679.

Papazachos B. C. and Papazachou C. 2003. *The earthquakes of Greece*, Ziti publications, Thessaloniki, 289 pp.

Paradisopoulou P.M., Papadimitriou E.E., Karakostas V.G., Taymaz T., Kilas A., and Yolsal S. 2010a. Seismic hazard evaluation in western Turkey as revealed by stress transfer and time-dependent probability calculations, *Pure and Applied Geophysics* doi: 10.1007/s00024-010-0085-1.

Paradisopoulou P.M., Papadimitriou E.E., Karakostas, V.G., Lasocki S., Mirek J. and Kilias A. 2010b. Influence of stress transfer in probability estimates of M≥6.5 earthquakes in Greece and surrounding areas 2010, *Bulletin of the Geological Society of Greece,* XLIII, 2114–2124.

Parsons T. 2004. Recalculated probability of M≥7 earthquakes beneath the Sea of Marmara, Turkey, *Journal of Geophysical Research,* 109, doi:10.1029/2003JB002667.

Parsons T. 2005. Significance of stress transfer in time–dependent earthquake probability calculations, *Journal of Geophysical Research,* 110, doi: 10.1029/2004JB003190.

Parsons T., Toda S., Stein R. S., Barka A. and Dieterich J.H. 2000. Heightened odds of large earthquakes near Istanbul: An interaction–based probability calculation, *Science,* 288, 661–665.

Pavlides S.B., Valkaniotis S., Ganas A., Keramydas D. and Sboras S. 2004. The Atalanti active fault: re-evaluation using new heological data, *Bulletin of the Geological Society of Greece* vol. XXXVI, *Proceedings of the 10th International Congress*, 1560-1567, Thessaloniki.

Pondard N., Armijo R., King, G. C. P., Meyer B. and Flerit F. 2007. Fault interactions in the Sea of Marmara pull–apart (North Anatolian Fault): earthquake clustering and propagating earthquake sequences, *Geophysical Journal International,* 171, 1185–1197.

Robinson R. and McGinty P.J. 2000. The enigma of the Arthur's Pass, New Zealand, earthquake. 2. The aftershock distribution and its relation to regional and induced stress fields, *Journal of Geophysical Research,* 105, 16139-16150.

Rockwell T., Barka A., Dawson T., Akyuz S. and Thorup K. 2001. Paleoseismology of the Gazikoy–Saros segment of the North Anatolia fault, northwestern Turkey: Comparison of the historical and paleoseismic records, implications of regional seismic hazard and models of earthquake recurrence, *Journal of Seismology,* 5, 433–448.

Stein R.S., Barka A.A. and Dieterich J.D. 1997. Progressive failure on the North Anatolian fault since 1939 by earthquake stress triggering, *Geophysical Journal International,* 128, 594-604.

Toda S., Stein R.S., Reasenberg P.A. and Yoshida A. 1998. Stress transferred by the 1995 Mw=6.9 Kobe, Japan shock: Effect on aftershocks and future earthquake probabilities, *Journal of Geophysical Research,* 124, 439-451.

Working Group on California Earthquake Probabilities (WGCEP), 1990. Probabilities of large earthquakes in the San Francisco Bay region, California, *U.S. Geol. Surv. Circ.* 1053, 51pp.

Working Group on California Earthquake Probabilities (WGCEP), 1999. Probabilities of large earthquakes in the San Francisco Bay region, California, *U.S. Geological Survey, Open File Report,* 99-517.